Availability, dynamics and chemistry of groundwater in the Bucklige Welt region of Lower Austria

Sebastian PFLEIDERER[1),*)], Heinz REITNER[1)] & Albrecht LEIS[2)]

[1)] Geological Survey of Austria, Neulinggasse 38, 1030 Vienna, Austria;

[2)] JR-AquaConSol GmbH, Steyrergasse 21, 8010 Graz, Austria;

[*)] Corresponding author, sebastian.pfleiderer@geologie.ac.at

Abstract

The Bucklige Welt region in the south-eastern part of Lower Austria experiences occasional shortages in the local water supply during dry periods. Until now a detailed investigation of existing aquifers and their hydrological or hydrochemical characteristics in this region has been lacking. Therefore, a study was carried out to characterise the availability, dynamics and chemistry of shallow groundwater. Collected data include (a) in-situ measurements of discharge (Q) and the physico-chemical parameters water temperature (WT), electrical conductivity (EC) and pH at 747 springs, (b) river discharge measured within a period of dry weather conditions at 59 sites, (c) in-situ measurements of Q, WT, EC and pH and chemical analyses of major ion concentrations of 135 groundwater samples taken within a period of dry weather conditions, (d) in-situ measurements of Q, WT, EC and pH, chemical analyses of major ion and trace element concentrations and ^{18}O isotope analyses of 529 water samples collected monthly at 43 springs and three wells over twelve months and (e) in-situ measurements of Q, WT and EC at two springs recorded at 15 minute intervals over a period of six months.

The study area is predominantly composed of mica schist, Augen gneiss and paragneiss, which provide low groundwater yields (1.5 to 6.2 L/s/km²). Locally, areas of calc-mica schists and quartzites yield more groundwater (26 and 31.8 L/s/km², respectively). The most productive aquifers constitute Quaternary valley sediments, which currently cover the water demand of larger settlements. Apart from the sediment aquifers, groundwater occurrences represent shallow fracture aquifers with small recharge areas and highly variable discharge over time. Base flow can increase by a factor of 6 after the snow melt and by a factor of up to 10 in months of high precipitation. Mean groundwater residence times range from 14 to 21 months. Mineralisation is generally low (the sum of dissolved solids lies between 68 and 351 mg/L), only the occurrences of marble or calc-mica schists in catchment areas result in higher concentrations (395 to 539 mg/L). Austrian national guideline values for drinking water are occasionally exceeded with respect to Na$^+$, Cl$^-$, NO$_3^-$, Fe^{2+}, Mn^{2+}, Al and Ni. Among these parameters, elevated concentrations of Na$^+$, Cl$^-$, NO$_3^-$ and Ni are considered to be of anthropogenic origin, and Fe^{2+}, Mn^{2+} and Al of geogenic origin.

Our results demonstrate the lack of new potential groundwater resources in the study area. Furthermore, the existing groundwater resources, while of good quality, are shown to exhibit a strong dependency on weather conditions. Based on these findings, local water authorities are currently planning to secure a sustainable supply of drinking water by tapping into aquifers outside the study area.

In der Buckligen Welt im südöstlichen Niederösterreich kommt es während längerer Trockenperioden zu Versorgungsengpässen bei der lokalen Trinkwasserversorgung. Bisher liegen für das Gebiet flächendeckend keine detaillierten Studien über die Grundwasservorkommen und deren hydrologische oder hydrochemische Eigenschaften vor. Die vorliegende Studie wurde durchgeführt, um das Dargebot, die Dynamik und die Chemie der oberflächennahen Grundwässer zu beschreiben. Die zugrundeliegenden Daten beinhalteten (a) In-situ-Messungen der Quellschüttung (Q) und der physiko-chemischen Parameter Wassertemperatur (WT), elektrische Leitfähigkeit (EC) und pH an 747 Quellen, (b) Abflussmessungen an 59 Oberflächengerinnen während einer Trockenperiode, (c) In-situ-Messungen von Q, WT, EC und pH sowie Bestimmung der Hauptionengehalte von 135 Grundwasserproben, die während einer Trockenperiode gezogen wurden, (d) In-situ-Messungen von Q, WT, EC und pH sowie Bestimmung der Hauptionengehalte, Spurenelementgehalte und ^{18}O-Gehalte von 529 Grundwasserproben, die über elf Monate an 43 Quellen und 3 Brunnen monatlich gezogen wurden und (e) In-situ-Messungen von Q, WT und EC an zwei Quellen in 15-minütigen Intervallen während eines Zeitraumes von sechs Monaten.

Das Gebiet ist hauptsächlich aus Glimmerschiefern, Augengneisen und Paragneisen aufgebaut, deren Grundwasserdargebot geringe Abflussspenden aufweist (1,5 bis 6,2 L/s/km²). Lokale Vorkommen von Kalkglimmerschiefern und Quarziten ergeben höhere Abflussspenden von jeweils 26 und 31,8 L/s/km². Die ergiebigsten Grundwasservorkommen treten in quartären Talfüllungen auf, die derzeit auch die Trinkwasserversorgung von größeren Ortschaften gewährleisten. Abgesehen von Grundwässern in Lockersedimenten handelt es sich bei den Aquiferen um seichte Kluftgrundwasserkörper mit kleinen Einzugsgebieten und zeitlich stark variierender Wasserführung. Der Basisabfluss von Quellen kann während der Schneeschmelze um das sechsfache, in regenreichen

Perioden um das zehnfache ansteigen. Mittlere Verweilzeiten der Grundwässer betragen zwischen 14 und 21 Monaten. Die Gesamtmineralisation ist generell niedrig (Summe der gelösten Stoffe zwischen 68 und 351 mg/L), in Einzugsgebieten mit Vorkommen von Marmor oder Kalkglimmerschiefern werden höhere Werte erreicht (395 – 539 mg/L). Gemäß der österreichischen Trinkwasserverordnung werden die Grenzwerte für Trinkwasser gelegentlich bei Na^+, Cl^-, NO_3^-, Fe^{2+}, Mn^{2+}, Al und Ni überschritten. Dabei erscheinen erhöhte Gehalte an Na^+, Cl^-, NO_3^- und Ni anthropogen, erhöhte Gehalte an Fe^{2+}, Mn^{2+} und Al geogen bedingt.

Die Studie bestätigt, dass im Untersuchungsgebiet kein Potenzial für zusätzliche Grundwasserressourcen besteht. Zusätzlich wird aufgezeigt, dass die existierenden Grundwasservorkommen zwar von guter Qualität aber stark witterungsabhängig sind. Als Folge der vorliegenden Arbeit haben die lokalen Wasserversorger beschlossen, für die nachhaltige Versorgung mit Trinkwasser auf Grundwasservorkommen außerhalb des Untersuchungsgebietes zurückzugreifen.

1. Introduction

The Bucklige Welt region, situated 75 km south of Vienna in the south-eastern part of Lower Austria, is characterised by low annual precipitation rates (700 – 850 mm; Skoda and Lorenz, 2003) and experiences occasional shortages in the local water supply during dry periods (Neunteufel et al., 2016). Furthermore, climate change forecasts suggest that these dry periods and shortages may become more frequent in the future (Formayer et al., 2015; Haslinger et al., 2016). Therefore, water authorities in the Bucklige Welt region are seeking new ways to guarantee a sustainable supply of drinking water. Consequently, there is a need to identify and characterise potential groundwater resources to improve the water supply.

Until now a detailed analysis of aquifers in the Bucklige Welt region (Austrian groundwater bodies GK100180 "Bucklige Welt – Raab / Rabnitz" and GK100086 "Bucklige Welt – Leitha") and their hydrological or hydrochemical characteristics has been lacking. Existing hydrogeological maps and studies either offer broad overviews (Schubert et al., 2003; Hobiger and Klein, 2004; Hobiger et al., 2007), or only cover small parts of the area in detail (Habart, 1978 and 1981; Suette and Zojer, 2005). Of the Austrian monitoring network for groundwater quality, only one station is located in the study area (BMLFUW, 2014). In order to assess potential groundwater resources in the Bucklige Welt region, a study was carried out to characterise the availability, dynamics and chemistry of groundwater within shallow aquifers. The results presented here are based on this study (Pfleiderer et al., 2015).

Geologically, the area is mainly composed of mica schist, Augen gneiss, paragneiss and, to a lesser extent, calc-mica schist (Figure 1). With respect to groundwater yield and storage, these rock types do not constitute hopeful candidates for large groundwater resources. For individual farms, the current water supply is centred primarily on springs of low yield (< 0.5 L/s) and wells of shallow depth (< 5 m). 60 % of the springs and 50 % of the wells are located in gneiss areas, 20 % of the springs occur in Neogene sediments (Krumbach formation) of the Norian depression (source: Wasserdatenverbund NÖ). Water demand of larger settlements, e.g. Krumbach or Kirchschlag, is covered by wells of higher yield situated in Quaternary valley sediments. At Bad Schönau, thermal groundwater is pumped from several wells of maximal 590 m depth, and used for balneological purposes (Kriegl and Goldbrunner, 2001).

Apart from the thermal groundwater occurrence, the groundwater reservoirs currently used exhibit small recharge areas, high vulnerability and a critical dependence on short term recharge during snow melt and rainy periods. The purpose of this paper is to present quantitative estimates of yield, flow dynamics, residence times, mineralisation and trace element concentrations of shallow groundwater occurrences in the study area. These estimates are intended to be used as a basis for future water supply and management measures.

2. Field measurements and analytical methods

The study area covers a surface area of 355 km². A compilation of geological maps at the scale of 1:50,000 (Herrmann et al., 1982 and 1992; Fuchs et al., 1995; Nowotny et al., 2002; Kreuss, 2015) served as a geological base map. Existing hydrological data (Wasserdatenverbund NÖ) were complemented by five newly acquired data sets.

a) A systematic mapping of springs and wells during summer months including measurements of spring discharge (Q) at 747 locations using the buckets-and-stop-watch method, and in-situ recordings of water temperature (WT), electrical conductivity (EC) and pH using WTW Type 340i and Type pH 330 instruments with SenTix 41, Tetra Con 325 and SenTix ORP electrodes.

b) The discharge of 59 small rivers was measured using the salt-tracer-dilution method. The measurements were taken in late autumn within a period of two days preceded by three weeks of dry weather conditions across the entire study area. During the month preceding this dry period, three periods of 4 – 6 days with 6 – 16 mm of rainfall per day occurred, and precipitation totalled 140 – 170 mm.

c) Groundwater samples were taken in late autumn at 135 sites within a period of three days preceded by three weeks of dry weather across the entire study area. Weather conditions before this dry period were the same as for data set (b). Q, WT, EC and pH were recorded in-situ using the same methods as for data set (a). Samples were analysed for concentrations of Ca^{2+}, Mg^{2+}, Na^+, K^+, Fe^{2+}, Mn^{2+}, HCO_3^-, SO_4^{2-} Cl^- and NO_3^-.

d) 43 springs and three wells were monitored at monthly intervals over a period of twelve months (24 springs from November 2012 until October 2013; 19 springs and three wells from November 2013 until October 2014) resulting in 46 time series. Q, WT, EC and pH were recorded in-situ using the same methods as for data set (a). Discharge mea-
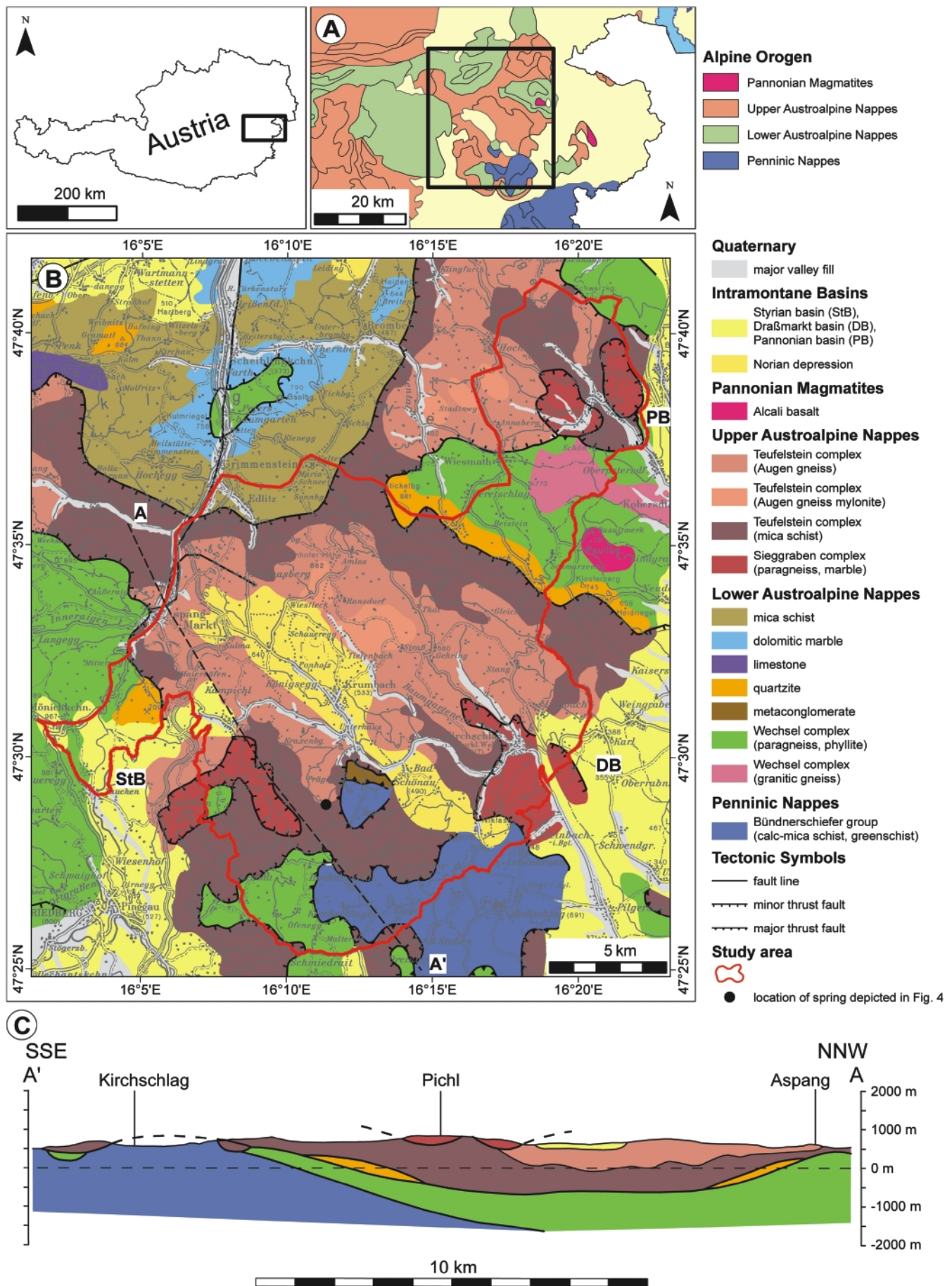
Figure 1: (A) Tectonic overview (Schuster, 2015); (B) Geological overview of study area (Schnabel et al., 2002 modified according to Schuster, 2015), Topography: © BEV 2017, (C) Geological cross section (Wessely et al., 2006, adapted).

surements were only carried out for the 43 springs. In total, 529 water samples were analysed for concentrations of Ca^{2+}, Mg^{2+}, Na^+, K^+, Fe^{2+}, Mn^{2+}, HCO_3^-, SO_4^{2-} Cl^-, NO_3^-, Al, As, Ba, Cd, Co, Cr, Cs, Cu, F, Li, Mn, Mo, Ni, Pb, Rb, Sr, U, V and Zn. In addition, ^{18}O was measured for the same samples using a Finnigan Delta^{plus} mass spectrometer coupled to a fully automated CO_2 equilibration device adapted from Horita et al. (1989).

e) At two springs, water levels were recorded at 15 minute intervals for a period of six months using sensors placed in rectangular weirs immediately downstream of the springs. Water levels were converted to discharge. For each spring, the conversion was calibrated with seven discharge measurements using the buckets-and-stop-watch method. In addition, WT and EC were recorded using the same methods as for data set (a). All recordings were captured with data loggers.

For data sets (c) and (d), water sampling, preservation and handling were carried out according to ÖNORM EN ISO 5667 (Austrian Standards Institute, 2013). Cation concentrations were measured using an Agilent Technologies Type 7500 mass spectrometer with inductively coupled plasma taking multiple measurements according to DIN EN ISO 17294-2. Concentrations of HCO_3^- were determined using a Mettler Toledo T70 titrator according to DIN 38409-H7-1-2 (DEV). All other anion concentrations were determined using a DIONEX Type ICS-2000 ion-chromatograph with suppressor technique and taking multiple measurements according to DIN EN ISO 10304-1. Quantification limits amounted to 10 mg/L for HCO_3^-, 0.5 mg/L for Cl^-, NO_3^- and SO_4^{2-} and 0.05 mg/L for F^-. Quantification limits amounted to 0.05 mg/L for K^+, 0.01 mg/L for Ca^{2+} and Na^+, 0.001 mg/L for As, Fe^{2+}, Mg^{2+}, Sr^{2+} and Zn, and 0.0001 mg/L for Al, Ba^{2+}, Cd, Cr, Cs^+, Co, Cu, Li^+, Mn^{2+}, Mo, Ni, Pb, Rb^+, U and V.

For ^{18}O measurements of data set (d), the analytical error amounted to ± 0.05 ‰ $\delta^{18}O$. For the calculation of groundwater residence times, the input signal was derived from isotope data of four ANIP stations (Austrian Network of Isotopes in Precipitation; Kralik et al., 2003). Modelling of residence times was carried out using the sine-wave approach (McGuire and McDonnell, 2006: equations 10). Results were calculated assuming an exponential as well as a dispersive flow model (McGuire and McDonnell, 2006: equations 12 and 14, respectively).

As statistical methods, linear correlation analysis, univariate and multivariate analysis of variance (ANOVA, MANOVA) were performed on major ion concentrations (in meq/L) of data set (c). Outliers and extreme val-

ues of trace element concentrations (in mg/L) of data set (d) were identified using the two-sided Tukey test (Tukey, 1977). The Tukey method tests whether a data value is larger than $q_{75}+c(q_{75}-q_{25})$ or smaller than $q_{25}-c(q_{75}-q_{25})$. For outliers, a coefficient of c = 2 was used, for extreme values c = 3. As the data distributions were skewed, symmetric distributions were obtained through log-transformations of the data prior to the analyses. A prerequisite of all these methods is a normal distribution of data. Therefore, the Kruskall-Wallis test was performed as a non-parametric method on major ion concentrations (in meq/L) of data set (c). For ANOVA, MANOVA and the Kruskall-Wallis test, major ion concentrations represented the dependent variables, rock types the independent variable.

3. Results

3.1 Groundwater availability

Table 1 shows statistical parameters of spring discharge measurements, irrespective of the size or the geological background of the spring catchment area. Discharge is generally low (median: 0.07 L/s), 75 % of all the springs yield less than 0.15 L/s. Table 1 lists medians since the data are not normally distributed. During dry periods, the sum of all spring waters within a catchment area can be approximated by the discharge of rivers. Figure 2 illustrates the discharge of 59 rivers related to the size of the catchment areas. Hydrological catchments were delineated on the basis of surface morphology. Yields per unit area are classified according to natural breaks (Jenks, 1967). In the study area, the values typically range from 0.8 to 7.6 L/s/km² with 86 % of values below 5 L/s/km². Only three catchments reach higher values (Tiefenbach: 11.2 L/s/km², Schwarzenbach: 18.5 L/s/km² and Kirchschlag: 19.3 L/s/km²). Conclusions on the availability of groundwater specific to geo-

	count	min	q25	median	q75	max
captured springs	174	0.003	0.03	0.08	0.16	2.5
un-captured springs	573	0.002	0.04	0.07	0.15	2.0

Table 1: Statistical parameters of spring discharge measurements (L/s).

geological unit	main lithology	number of springs per unit	yield per unit area (L/s/km²)
Styrian basin	loamy sand with boulders	7	3.60
Norian depression	clay and silt with sandy layers	10	3.21
Sieggraben complex	paragneiss	7	1.93
Teufelstein complex	Augen gneiss	39	3.14
	Augen gneiss mylonite	8	3.48
	mica schist	26	4.02
-	mica schist	1	*6.16*
	quartzite	1	*31.81*
	metaconglomerate	1	*3.15*
Wechsel complex	paragneiss	19	2.09
	granitic gneiss	5	1.46
Bündnerschiefer group	calc-mica schist	1	*25.97*
	greenschist	3	1.56

Table 2: Groundwater yields derived from spring discharge. Medians of yield per unit area for geological units occurring in the study area. Geological units according to Figure 1 (Schuster, 2015). Values in italics are based on one spring only.
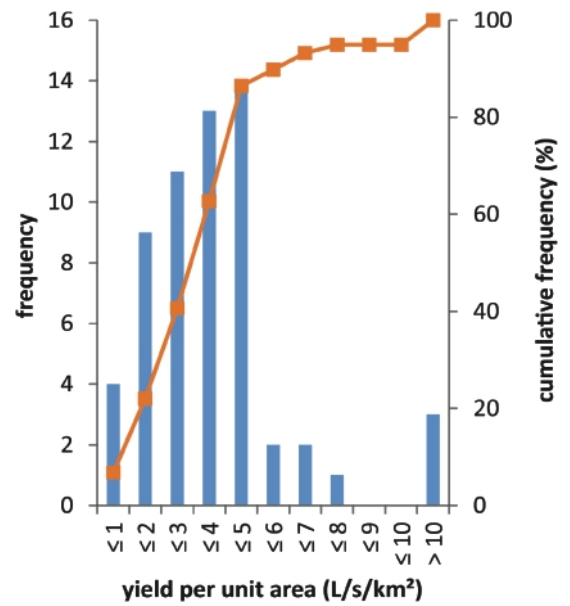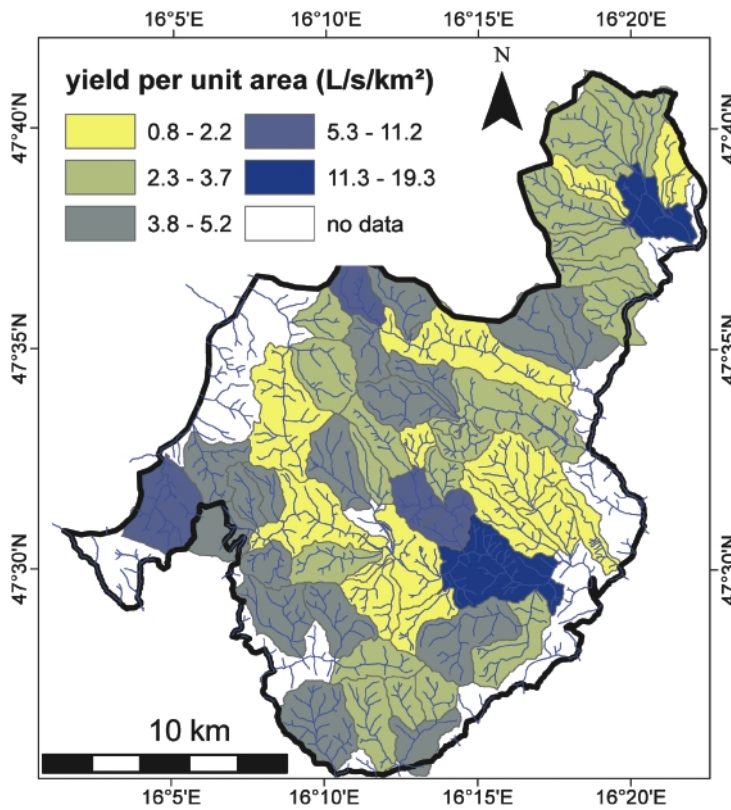
Figure 2: Groundwater yields derived from river discharge. Regional distribution (left) and frequency distribution (right) of yield per unit area for 59 catchment areas.

logy cannot be drawn from this dataset since most of the catchment areas cover more than one geological unit.

Groundwater yields of specific geological units are presented in Table 2. The yields per unit area of 128 springs with geologically homogenous catchments are grouped by geological units in this table. The number of springs within each unit is also given. For units containing more than one spring, the median is listed. The yields generally range from 1.5 to 6.2 L/s/km². Only springs draining areas of calc-mica schists and quartzites display higher values (26 and 31.8 L/s/km² respectively). Comparable to the data derived from river discharge (Figure 2), 69 % of values stay below 5 L/s/km².

3.2 Groundwater flow dynamics and residence times

Figure 3 shows an example of the time series of twelve monthly measurements of spring discharge and electrical conductivity. Rainfall at the nearest rain monitoring station during the three weeks preceding each measurement is also given. Increases of base flow by a factor of 6 after the snow melt (February 2014), and by a factor of 3 to 10 in months of high precipitation (September and May 2014 respectively), are visible. The recordings of the months following these peaks (March, June and October 2014) show that discharge has receded back to base level. Spring discharge variations are mirrored by changes in electrical conductivity with high discharge being accompanied by low electrical conductivity, i.e. decrease in mineralisation through mixing with rainwater. In order to quantify the dynamics of springs, the relative inter-percentile deviation (RID) was calculated for each time series of monthly measurements of discharge. RID was calculated as q90 – q10 as a per-
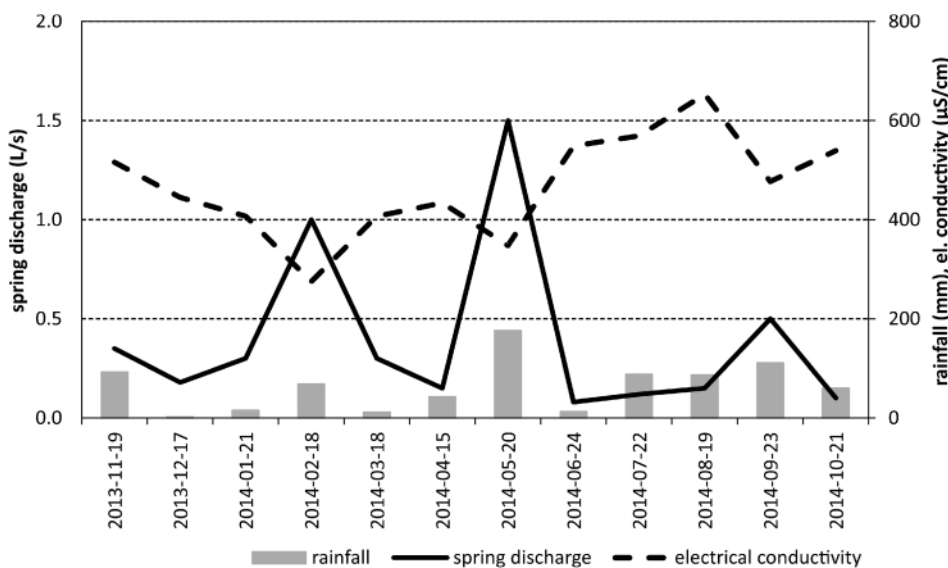

Figure 3: Monthly measurements of spring discharge and electrical conductivity (one example of 43 springs). Rainfall represents the sum of rain during three weeks preceding the measurements.

centage of q50 (Kralik, 2001). The data in Figure 3 represent the dynamics of a spring with a catchment composed of Augen gneiss. RID amounts to 375, i.e. discharge is highly variable. In Table 3, RID values of 43 time series are summarised for each geological unit. For units containing more than one spring, the median is listed. Dynamics of spring discharge are high or extremely high (RID > 200 or > 270, respectively) within most geological units. Only one spring within an area of quartzites shows a less dynamic behaviour (RID ≤ 200).

Measurements of discharge and temperature at 15 minute intervals were carried out at two springs in order to study groundwater flow dynamics at a high time resolution. Figure 4 shows the data for one of the two springs which drains a catchment area composed of Augen gneiss. Discharges range from 0.24 to 1.9 L/s. During 3 – 4 consecutive days of rainfall (14 – 16 mm per day from Aug 31 to Sep 2), spring discharge increases sevenfold. It takes up to 2 weeks without rainfall for the level to start receding again.

geologic unit	main lithology	time series count	RID	dynamics
Styrian basin	loamy sand with boulders	2	379	extremely high
Norian depression	clay and silt with sandy layers	7	230	high
Sieggraben complex	paragneiss	3	340	extremely high
Teufelstein complex	Augen gneiss	8	436	extremely high
	Augen gneiss mylonite	4	398	extremely high
	mica schist	5	412	extremely high
-	quartzite	1	*130*	*medium*
	mica schist	1	*257*	*high*
Wechsel complex	paragneiss	6	326	extremely high
	granitic gneiss	1	*1235*	*extremely high*
Bündnerschiefer group	calc-mica schist	3	336	extremely high
	greenschist	2	225	high

Table 3: Dynamics of spring discharge as expressed by the relative inter-percentile deviation (RID). Medians of RID for geological units occurring in the study area. Values in italics are based on one time series only.
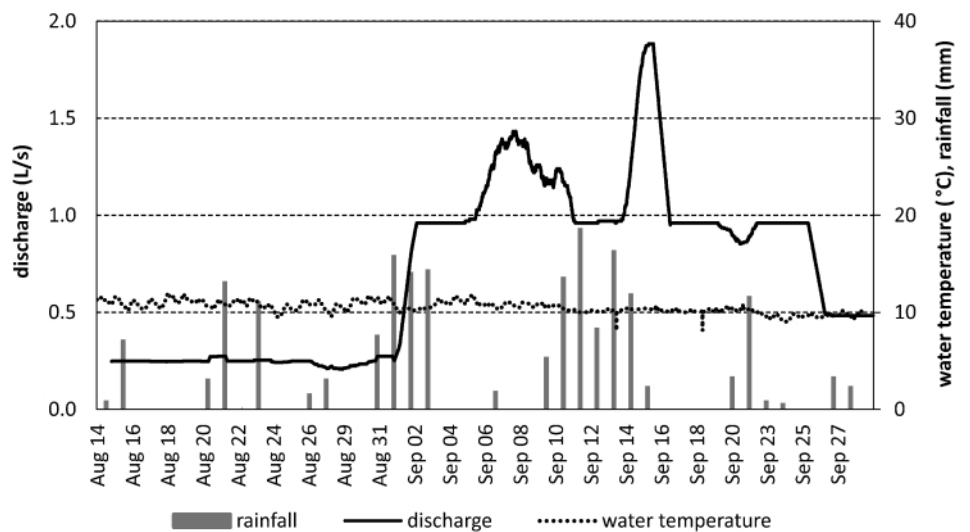

Figure 4: Daily rainfall and continuous measurements of discharge (averaged over 24 hours) and temperature at a spring which drains an area of Augen gneiss (location depicted in Figure 1).

The daily variations of water temperature, which reflect changes in air temperature, are less pronounced during this time. A similar effect of short term rainfall on discharge was observed at the second spring located in a paragneiss area. There, during a similar rain event, discharge increases by a factor of 2.5 and starts subsiding after one week.

Groundwater residence times were evaluated on the basis of water ^{18}O isotope measurements. Fitting a sine-wave to

geological unit	main lithology	number of sites per unit	mean groundwater residence time		
			min	median	max
Quaternary valley fill	sandy gravel	2	15.8	18.3	20.7
Styrian basin	loamy sand with boulders	3	10.3	18.3	20.7
Norian depression	clay and silt with sandy layers	7	11.0	17.8	20.4
Sieggraben complex	paragneiss	3	13.7	14.3	17.2
Teufelstein complex	Augen gneiss	8	4.6	16.5	19.8
	Augen gneiss mylonite	4	14.6	18.8	19.9
	mica schist	5	10.4	16.5	19.4
-	quartzite	1	18.7	18.7	18.7
	mica schist	1	16.3	16.3	16.3
Wechsel complex	paragneiss	6	16.1	17.3	20.2
	granitic gneiss	1	14.3	14.3	14.3
Bündnerschiefer group	calc-mica schist	3	19.2	19.2	25.0
	greenschist	2	18.1	20.7	23.3

Table 4: Mean groundwater residence times in months, derived from δ^{18}O variations of 475 water samples taken monthly at 46 sites, grouped by geological unit.

annual $\delta^{18}O$ variations in rainfall over five years reveals an amplitude of 2.91 ‰. By comparison to time series of monthly groundwater samples, amplitude damping factors were calculated for 43 springs and 3 wells. These damping factors were then used to derive mean groundwater residence times according to both an exponential and a dispersive groundwater flow model. For the dispersive model, a Péclet number of 40 was used. This results in 80 % (q10 – q90) of all mean residence times ranging between 14 and 21 months. Table 4 lists the results for the dispersive model, grouped by geological units of the catchments. Springs or wells draining unconsolidated sediments (Quaternary valley fill, Styrian basin, Norian depression), as well as springs draining mylonites, quartzites, greenschists and calc-mica schists, display the highest values (medians of residence times within geological units $\geq$17.8 months). Results for the exponential model show substantially larger variations (80 % of data ranging from 6 to 32 months).

3.3 Groundwater chemistry

Figure 5 shows the concentrations of major ions, Fe^{2+} and Mn^{2+} of 135 groundwater samples collected across the study area. With respect to the Austrian national guideline values for drinking water (Trinkwasserverordnung 2001), one sample exceed the limits for Na^+ and Cl^-, five samples for Fe^{2+}, 13 samples for Mn^{2+} and nine samples for NO_3^-. Linear correlation analysis reveals high coefficients of determination ($r^2 > 0.5$) between EC, Ca^{2+} and Mg^{2+} concentrations, between Ca^{2+}, Mg^{2+} and HCO_3^- concentrations, and between Na^+ and Cl^- concentrations (Table 5).

The sums of dissolved solids (TDS = Ca^{2+} + Mg^{2+} + Na^+ + K^+ + HCO_3^- + SO_4^{2-} + Cl^- + NO_3^- in mg/L) of the same 135 samples show a bimodal distribution with concentrations of one group of samples ranging between 30 and 251 mg/L and a second group between 301 and 630 mg/L. TDS concentrations are listed in Table 6, grouped by geological units of the springs' catchments. Spring waters with slightly elevated mineralisation (median of TDS > 395 mg/L) can be identified within the Sieggraben complex in areas of marble occurrence, in metaconglomerates and in calc-mica schists.

Figure 6 simultaneously shows the regional distribution and ternary plots of ionic composition of the same samples. This figure combines the graphical representation commonly used in Piper diagrams, with the presentation of point symbols on maps (Hamilton et al., 2015). Anions and cations are plotted separately in ternary plots over a Maxwell colour triangle (Chamberlin and Chamberlin, 1980) and the RGB values for each ionic composition are then used to colour the point symbols on the maps. For orientation, the centre map displays geological units (as in Figure 1). Thus, it is possible to examine multivariate chemical compositions specific to geological units. Figure 6 reveals that the populations of data points specific to geological units overlap in the ternary plots and show similar colours across the maps. There are, however, three exceptions. (1) The ionic composition of spring water within areas of calc-mica schists and of marbles show a dominance of Ca^{2+} over Mg^{2+} and over $Na^+ + K^+$, and a dominance of HCO_3^- over SO_4^{2-} and over Cl^- (red colours). (2) Anion
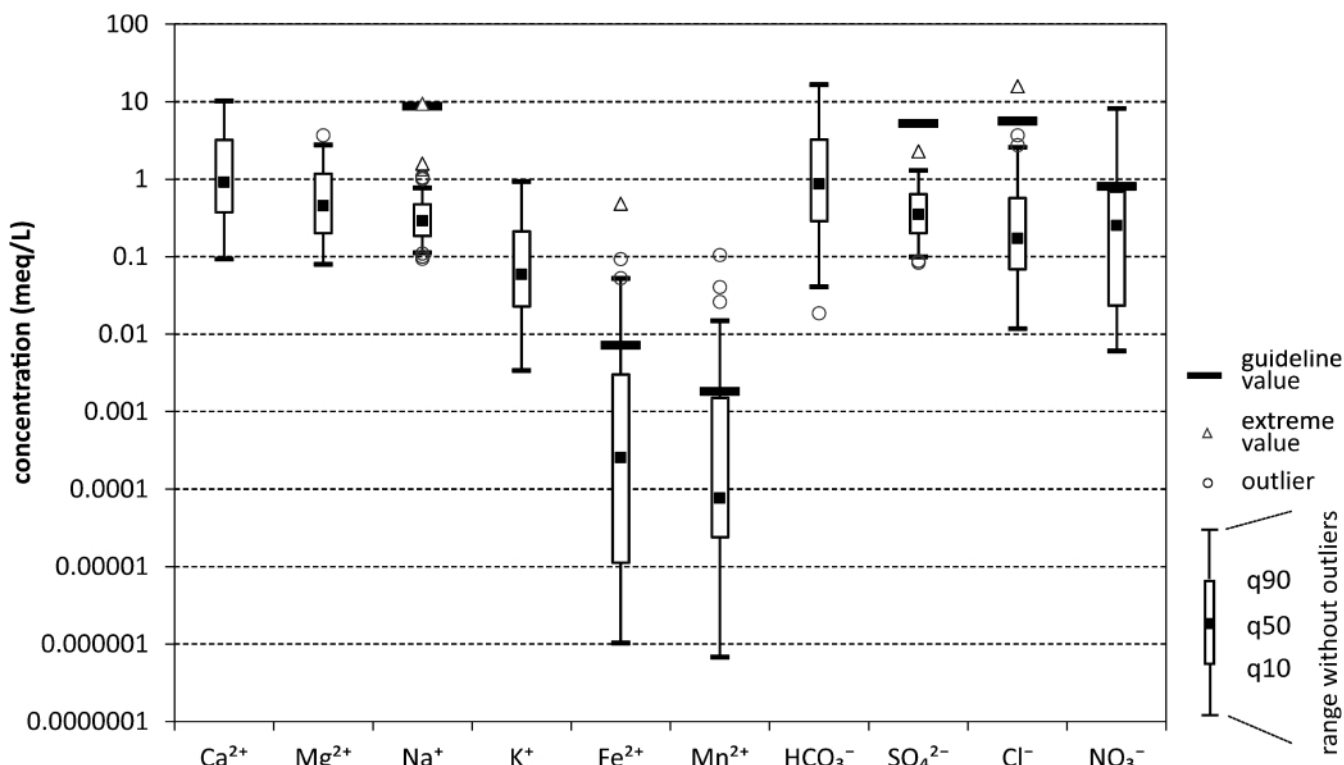

Figure 5: Box-and-whiskers plot of major ion concentrations (including Fe^{2+} and Mn^{2+}) of 135 groundwater samples collected within a period of dry weather conditions.

compositions strongly dominated by SO_4^{2-} (blue colours) occur in spring water within the Styrian basin. (3) Green coloured symbols highlight samples with a Na^+ dominance in cationic composition or a Cl^- dominance in anionic composition. Sampling points where the two coincide, i.e. high concentration of dissolved rock salt, are located near major roads.

	Ca^{2+}	Mg^{2+}	Na^+	K^+	HCO_3^-	SO_4^{2-}	Cl^-	NO_3^-
EC	**0.5630**	**0.5640**	0.4617	0.1058	0.3365	0.2729	0.4621	0.0399
Ca^{2+}		**0.8109**	0.1715	0.0676	**0.7901**	0.2156	0.3298	0.1118
Mg^{2+}			0.2513	0.0930	**0.6559**	0.2338	0.3860	0.1096
Na^+				0.1769	0.0871	0.1274	**0.6939**	0.0275
K^+					0.0736	0.0438	0.1123	0.0870
HCO_3^-						0.0867	0.1368	0.0175
SO_4^{2-}							0.1023	0.0304
Cl^-								0.1269

Table 5: Coefficients of determination (r^2) between electrical conductivity (EC) and major ion concentrations of 135 groundwater samples. Values of $r^2 > 0.5$ in bold.

Regarding the relation between groundwater ionic composition and aquifer lithology, ANOVA results show statistically highly significant differences among the rock types of Table 6 for the concentrations of Ca^{2+}, Mg^{2+}, K^+ and HCO_3^-. F-values amount to 3.154, 3.051, 2.9182 and 3.200, respectively, with $p \leq 0.005$ (Table 7). MANOVA results indicate that the combination of these variables is statistically highly different among rock types. Results of the Kruskall-Wallis test confirm Ca^{2+}, Mg^{2+}, K^+ and HCO_3^- concentrations as the four most significant variables for differentiating between rock types (Table 7). H-values amount to 42.157, 44.109, 51.1425 and 42.226, respectively, with $p \leq 0.005$.

Concentrations of trace elements in 529 water samples collected at monthly intervals at 43 springs and 3 wells are shown in Figure 7. With respect to the Austrian national guideline values for drinking water (Trinkwasserverordnung 2001), one spring exceeds the limit for Al for all of the monthly water samples, and one spring and one well occasionally exceed the limit for Ni. In general, trace element concentrations are low and stay well below guideline values. Natural background levels derived for the wider area of south-eastern Austria by Hobiger and Klein (2004) (groundwater bodies Leitha and Raab,) are frequently exceeded in the study area with respect to Al, Cu and Ni concentrations whereas As, Cr and Pb concentrations stay well below natural background levels.

4. Discussion

Within the study area, the compilation of geological map sheets at the scale of 1:50,000 contains 52 geological units,
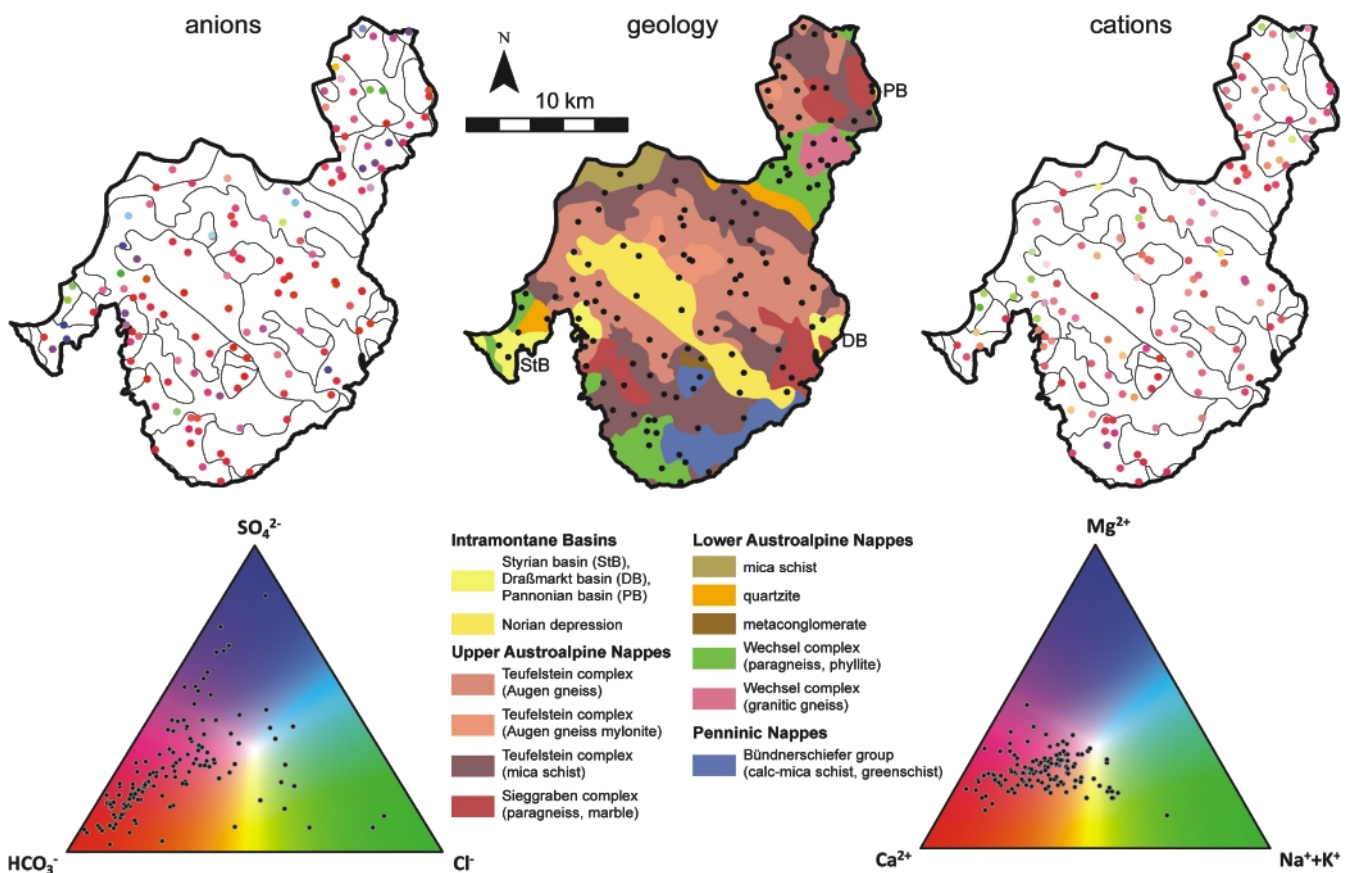

Figure 6: Regional distribution and ternary plots of ionic composition of 135 groundwater samples. Point symbol colours on maps correspond to colours in ternary plots.

each composed of a distinct lithology. Not all of these lithologies are covered by our hydrochemical data sets; 31 units contain no data points. Therefore, the lithologies were grouped into larger units according to lithology and tectonic setting (Figure 1) and conclusions were drawn specific to these units (Figure 6; Tables 2, 3 and 4). However, this grouping brings the disadvantage that some lithological differences within units, e.g. in areas of calc-mica schists within the Bündnerschiefer group or of marble occurrences within the Sieggraben complex, cannot then be resolved. Therefore, the geological base map 1:50,000 was used for the site-specific interpretation of individual springs or catchment areas. This was of particular importance when interpreting groundwater yield, dynamics or hydrochemical data. In Table 6, certain units were ungrouped to show the effect of different lithologies on the mineralisation.

The geological overview in Figure 1 shows the extent of Quaternary sediments in major valleys within the study area. Groundwater yield in these sediments is higher than in surrounding crystalline rocks. According to water supply data (Wasserdatenverbund NÖ), many wells in Quaternary sediments offer high yields and cover the water demand of larger settlements, e.g. Krumbach or Kirchschlag for the time being (Neunteufel et al., 2016). Springs do not occur in Quaternary valley sediments and data on the hydrochemistry and $\delta^{18}O$ were derived from water samples collected in wells.

Within crystalline rocks, elevated groundwater yields occur in calc-mica schists and in quartzite (Table 2). While each of

these rock types is represented by only one spring in the study area and the statistical significance of the data is insufficient to generalise results, the yields may still be explained by aquifer lithology. Calc-mica schists exhibit augmented porosity due to the high solubility of $CaCO_3$ which leads to stronger yields (26 L/s/km²). The elevated yield (31.8 L/s/km²), medium dynamics (RID = 130) and long residence times (18.7 months) of groundwater within quartzites may be explained by the dense fracturing of these rocks. They display a highly fractured nature in outcrops and are even mined locally as a sand and gravel resource without the need for crushing.

The yields per unit area in Figure 2 and Table 2 serve as an indication of groundwater availability. After three weeks without rainfall across the entire study area, and 140 – 170 mm of rainfall during one month before this dry period, it is assumed that all river and spring discharge measurements represent base flow. However, without continuous hydrographs, this remains an assumption. The only publicly available hydrograph in the study area (Zöbernbach river at Kirchschlag; Wasserstandsnachrichten NÖ, 2015) does show that base flow is reached two to three weeks after a major rain event which supports the above-mentioned assumption. Individual catchment areas may yet differ with regard to the precipitation rates preceding the dry period in addition to the recharge, storage and recession processes. The differences in yield shown in Figure 2 and Table 2 may not only reflect different aquifer lithologies but also regional differences in precipitation.

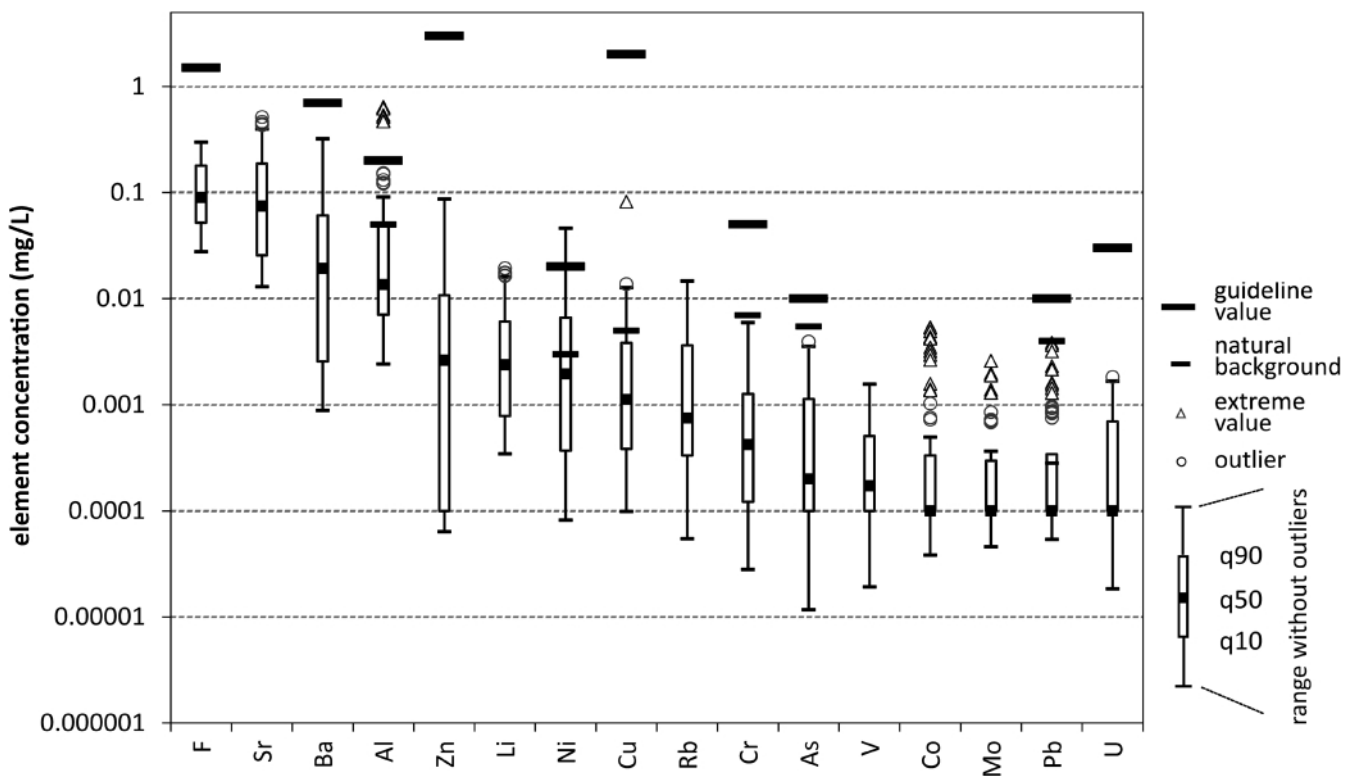Groundwater occurrences in the study area represent shallow

Figure 7: Trace element concentrations of 529 water samples collected at monthly intervals at 46 sites. Guideline values for drinking water according to the WHO (2011) for Ba, U, Zn and according to the Trinkwasserverordnung (2001) for other trace elements. Natural background levels according to Hobiger and Klein (2004).

aquifers with small recharge areas. This is evidenced by the time series of monthly ground-water temperature recordings which mirror the course of annual air temperature. Field measurements taken during the systematic mapping of springs and wells during summer months reveal a median groundwater temperature of 12.4 °C. The variations of discharge and electrical conductivity during rainy periods (Figure 3) and the dynamics of spring discharge during short-term precipitation events (Figure 4) provide further evidence for this.

According to Maloszewski & Zuber (1996), seasonal variations of $\delta^{18}O$ can be used to derive mean residence times of up to four years. The results in Table 4 range from 4.6 to 25 months, indicating that the use of this method is appropriate. However, no alternative isotope tracers, e.g. tritium, were studied and the results constitute only a first indication of residence times. The use and limitations of lumped parameter methods are discussed in detail by McGuire and McDonnell (2006). The sine-wave approach represents a simplification to estimate mean transit times. It has however the advantage that mean transit times of different springs in various parts of the investigation area can be derived in a comparable way.

- With regard to input signal characterization, the consideration of four ANIP stations and $\delta^{18}O$ time series covering five years reduced uncertainties in the calculation of the annual amplitude.
- The $\delta^{18}O$ signal in groundwater recharge was assumed to be represented by the isotopic composition of precipitation.
- The output signal was modelled on the basis of analyses of monthly water samples collected over 11 months at each site. Sampling sites were chosen such that the influence of infiltrating surface water near the sites could be excluded. The effect of short-term rain events was considered by observing the electrical conductivity of groundwater samples. In one case, the measured ^{18}O concentration of spring water exceeded the monthly precipitation value. This value was treated as an outlier and excluded from the dataset before the calculation of the mean residence time.
- The results of the exponential and the dispersion models were compared in order to test the assumption of transit time distribution. This revealed that the exponential model overestimates residence times in the case of strongly damped amplitudes. In two cases, results amounted to implausibly high residence times of 79.4 and 138.9 months, while in four other cases, results amounted to very low residence times between 1.1 and 3.9 months. Adopting a dispersion

geological unit	main lithology	sample count	total dissolved solids		
			min	median	max
Styrian basin	loamy sand with boulders	8	29.99	69.67	151.73
Norian depression	clay and silt with sandy layers	13	37.85	122.69	486.61
Sieggraben complex	granitic gneiss	1	*288.47*	*288.47*	*288.47*
	paragneiss	5	123.97	178.48	400.22
	marble	2	315.62	395.03	474.44
Teufelstein complex	Augen gneiss	31	63.53	147.54	1213.57
	Augen gneiss mylonite	5	75.12	117.28	143.85
	mica schist	34	35.92	123.73	438.69
	gabbro	1	*159.72*	*159.72*	*159.72*
-	quartzite	1	*237.33*	*237.33*	*237.33*
	mica schist	1	*108.94*	*108.94*	*108.94*
	metaconglomerate	2	453.06	538.90	624.75
Wechsel complex	paragneiss	22	61.30	164.32	629.76
	granitic gneiss	4	48.16	67.71	132.31
	amphibolite	1	*130.85*	*130.85*	*130.85*
Bündnerschiefer group	calc-mica schist	1	*447.22*	*447.22*	*447.22*
	greenschist	3	250.62	350.77	362.45

Table 6: Total dissolved solids (TDS in mg/L) of 135 groundwater samples grouped by geological units of the springs' catchment areas. Values in italics are based on one sample only.

	ANOVA		Kruskall-Wallis	
	F	p	H	p
Ca²⁺	**3.1543**	**0.0001**	**42.1567**	**0.0017**
Mg²⁺	**3.0511**	**0.0001**	**44.1085**	**0.0009**
Na⁺	1.8994	0.0204	35.4227	0.0124
K⁺	**2.9182**	**0.0002**	**51.1425**	**0.0001**
HCO₃⁻	**3.1999**	**0.0001**	**42.2263**	**0.0017**
SO₄²⁻	1.4055	0.1378	33.0901	0.0235
Cl⁻	1.9927	0.0137	31.0495	0.0399
NO₃⁻	2.2043	0.0055	33.2342	0.0226

Table 7: Results of ANOVA and the Kruskall-Wallis test showing the statistical significance of differences in major ion concentrations between rock types (135 groundwater samples, rock types listed in Table 6). Most significant variables ($p < 0.005$) in bold.

model led to a narrower range of residence times (14 – 21 months; section 3.2) and was therefore regarded as more appropriate. For groundwater flow through the fractured aquifers occurring in the study area, a Péclet number of 40 was chosen as a fitting parameter where the most reasonable results were obtained.

The chemical composition of groundwater samples is related to the lithology of the aquifers. The occurrence of marble or calc-mica schists in catchment areas results in elevated amounts of TDS (Table 6) and ionic compositions plotting in the far left corners of the Piper diagram (Figure 6) due to high concentrations of dissolved $CaCO_3$. Groundwater samples within the Styrian basin show a lower mineralisation (TDS = 70 mg/L) than samples from the Norian depression (TDS = 123 mg/L). This is due to the fact that sediments of the Styrian basin in the study area derive from a local crystalline source area while those of the Norian depression originate from an area stretching further west to the Calcareous Alps and consequently contain more carbonate components (Herrmann, 2008). The elevated mineralisation of groundwater in areas of metaconglomerate occurrence is not caused by the lithochemistry of these rocks but could be explained

by calc-mica schists which are adjacent to and underlie the metaconglomerates.

The statistical methods were applied in order to test if the rock types listed in Table 6 are statistically distinct with respect to groundwater chemistry. In Piper plots and grouped box plots, groundwater within marbles, calc-mica schists, metaconglomerates and paragneiss of the Wechsel complex can be clearly separated visually from the other rock types on the basis of Ca^{2+}, Mg^{2+} and HCO_3^- concentrations. The statistical tests quantitatively support these findings. Linear correlation analysis shows that these three parameters are strongly correlated. ANOVA identifies Ca^{2+}, Mg^{2+}, K^+ and HCO_3^- as highly significant variables for differentiating between rock types. However, sample counts for some of the rock types are too low for statistical analysis. In addition, these methods assume normal data distributions and homogeneity of variances. Even after log-transformation, outliers may still influence the results. Nevertheless, the non-parametric Kruskall-Wallis test also identifies Ca^{2+}, Mg^{2+}, K^+ and HCO_3^- as highly significant variables.

The elevated concentrations of Na^+ and Cl^- in groundwater are assumed to be due to road salt application since they simultaneously occur near major roads and no geological formation within the study area contains salt deposits. Equally, the ubiquitous occurrence of elevated NO_3^- concentrations is assumed to be of anthropogenic origin due to the use of fertilisers. In contrast, a geogenic origin is assumed for the elevated concentrations of Fe^{2+}, Mn^{2+} and Al. Data on stream sediment geochemistry (Pirkl et al., 2015) show very low levels of Ni in the study area. The localised occurrence of elevated Ni concentrations in groundwater points to an anthropogenic origin, potentially due to illegal waste dumps in ravines.

5. Conclusion

The Bucklige Welt region of Lower Austria is predominantly composed of mica schist, Augen gneiss and paragneiss which provide low groundwater yields (1.5 to 6.2 L/s/km^2). Sediments in the Styrian basin and the Norian depression also show low yields (3.6 and 3.2 L/s/km^2, respectively). Locally, areas of calc-mica schists and quartzites yield more groundwater (26 and 31.8 L/s/km^2, respectively). These areas, however, cover only small parts of the study area and therefore do not offer relevant groundwater resources for this region's water supply. Consequently, the quaternary valley sediments which currently cover the water demand of larger settlements (Wasserdatenverbund NÖ), will remain the only local option for the supply of drinking water.

Except for the sediment aquifers, the groundwater occurrences represent shallow fracture aquifers with small recharge areas and highly variable discharge over time. After the snow melt and in months of high precipitation, the base flow of springs increases by a factor of 6 and 10, respectively. Spring discharge is also highly sensitive to short-term rain events. Mean groundwater residence times typically range between 14 and 21 months. This shows that the aquifers are strongly dependent on continuous precipitation and groundwater recharge, and prolonged periods of low precipitation (snow or rain) can jeopardise a sustainable water supply.

The chemical composition of groundwater is related to the lithology of the aquifers. Mineralisation is generally low (the sum of dissolved solids lies between 68 and 351 mg/L). Only the occurrences of marble or calc-mica schists in catchment areas result in higher concentrations (the sum of dissolved solids lies between 395 and 539 mg/L). In addition, trace element concentrations are low and generally stay below the Austrian national guideline values for drinking water (Trinkwasserverordnung 2001). These values are only occasionally exceeded with respect to Na^+, Cl^-, NO_3^-, Fe^{2+}, Mn^{2+}, Al and Ni. Among these elements, elevated concentrations of Na^+, Cl^-, NO_3^- and Ni are considered to be of anthropogenic origin, and Fe^{2+}, Mn^{2+} and Al of geogenic origin. In conclusion, the quality of existing groundwater resources is generally high and could be improved even further by the reduction of anthropogenic input of road salt and nitrate.

Concerning the issue of occasional shortages in the local water supply, this study demonstrates the lack of new potential groundwater resources in the study area. Furthermore, it shows that the existing groundwater resources, while of good quality, exhibit a strong dependency on weather conditions. On the basis of these findings, the water authorities in the Bucklige Welt region have taken a new approach and are planning to secure a sustainable supply of drinking water by tapping into aquifers outside the study area (Stadtnachrichten Kirchschlag. 2016, Gemeindenachrichten Bad Schönau, 2016).

References

Austrian Standards Institute, 2013. Water quality — Sampling — Part 3: Preservation and handling of water samples (ISO 5667-3:2012). Austrian Standards Institute, Wien, 57 pp.

BMLFUW, 2014. Wassergüte in Österreich Jahresbericht 2013. Bundesministerium für Land- und Forstwirtschaft, Umwelt und Wasserwirtschaft, Wien, 84 pp.

Chamberlin, G.J. and Chamberlin, D.G., 1980. Colour, its measurement, computation, and application. Heyden, London, 137 pp.

Formayer, H., Nadeem, I. and Anders, I, 2015. Climate Change Scenario: from Climate Model Ensemble to local indicators. in: Steininger, K., König, M., Bednar-Friedl, B., Kranzl, L., Loibl, W. and Prettenthaler, F. (eds). Economic Evaluation of Climate Change - Development of a Cross-Sectoral Framework and Results for Austria (COIN). Springer, Cham, 461 pp. http://dx.doi.org/10.1007/978-3-319-12457-5

Gemeindenachrichten Bad Schönau, 2016. Trinkwasserzukunft Bucklige Welt. Gemeindenachrichten, 3/16, 4.

Fuchs, G., Schnabel, W., Herrmann, P., Pahr, A. and Riedmüller, G., 1995. Geologische Karte der Republik Österreich 1:50.000, Blatt 106 Aspang-Markt. Geologische Bundesanstalt, Wien.

Habart, F., 1978. Zur Geologie und Hydrogeologie des unteren Pittentales (Niederösterreich). Doctoral Thesis, Universität Wien, 228 pp.

Habart, F., 1981. Zur Geologie und Hydrogeologie des unteren Pittentales. Mitteilungen der Gesellschaft der Geologie- und Bergbaustudenten in Österreich, 27, 87–116.

Hamilton, S.M., Grasby, S.E., McIntosh, J.C. and Osborn, S.G., 2015. The effect of long-term regional pumping on hydrochemistry and dissolved gas content in an undeveloped shale-gas-bearing aquifer in southwestern Ontario, Canada. Hydrogeology Journal, 23, 719–739. http://dx.doi.org/10.1007/s10040-014-1229-7

Haslinger, K., Schöner, W. and Anders, I., 2016. Future drought probabilities in the Greater Alpine Region based on COSMO-CLM experiments spatial patterns and driving forces. Meteorologische Zeitschrift, 25/2, 137–148. http://dx.doi.org/10.1127/metz/2015/0604

Herrmann, P., Pahr, A. and Erich, A., 1982. Geologische Karte der Republik Österreich 1:50.000, Blatt 137 Oberwart. Geologische Bundesanstalt, Wien.

Herrmann, P., Mandl, G.W., Matura, A., Neubauer, F., Riedmüller, G. and Tollmann, A., 1992. Geologische Karte der Republik Österreich 1:50.000 Blatt 105 Neunkirchen. Geologische Bundesanstalt, Wien.

Herrmann, P., 2008. Becken von Krumbach, Zöbern und Lehmbach. in: Fuchs, G., Herrmann, P., Pahr, A. and Schnabel, W. (eds.). Erläuterungen zu Blatt 106 Aspang-Markt. Geologische Bundesanstalt, Wien, 82 pp.

Hobiger, G. and Klein, P. (eds), 2004. Österreichweite Abschätzung von regionalisierten, hydrochemischen Hintergrundgehalten in oberflächennahen Grundwassserkörpern auf der Basis geochemischer und wasserchemischer Analysedaten zur Umsetzung der Wasserrahmenrichtlinie 2000/60/EG GeoHint. Geological Survey of Austria Internal Report, Geologische Bundesanstalt, Wien, 444 pp.

Hobiger, G., Kollmann, H. and Shadlau, S., 2007. Thermal- und Mineralwässer. in: BMLFUW (ed.), Hydrologischer Atlas Österreichs, 3. Lieferung, Kartentafel 6.6. Bundesministerium für Land- und Forstwirtschaft, Umwelt und Wasserwirtschaft, Wien.

Horita, J., Ueda, A., Mizukami, K. and Takatori, I., 1989. Automatic δD and $\delta^{18}O$ analyses of multi-water samples using H_2- and CO_2-water equilibration methods with a common equilibration set-up. International Journal of Radiation Applications and Instrumentation. Part A. Applied Radiation and Isotopes, 40, 801–805.

Jenks, G.F., 1967. The Data Model Concept in Statistical Mapping. International Yearbook of Cartography, 7, 186–190.

Kralik, M., 2001. Spring dynamics as a tool to evaluate Groundwater-Vulnerability. 7th conference on Limestone Hydrology and Fissured Media, Besancon 20-22 Sept 2001, Sci. Techn. Envir., Mém. H. S. 13, 215–218.

Kralik, M., Papesch, W. and Stichler, W., 2003. Austrian Network of Isotopes in Precipitation (ANIP): Quality assurance and climatological phenomenon in one of the oldest and densest networks in the world. in: IAEA (ed.), Isotope Hydrology and Integrated Water Resources Management, Conference & Symposium Papers, 23, 146–149.

Kreuss, O., 2015. Geofast Zusammenstellung ausgewählter Archivunterlagen der Geologischen Bundesanstalt 1:50.000 136 Hartberg. Geologische Bundesanstalt, Wien.

Kriegl, C. and Goldbrunner, J., 2001. Erschließungsbohrung Bad Schönau IV („Christophorus-Milleniumsquelle") Geologisch-technischer Abschlussbericht und Antrag auf Erteilung der wasserrechtlichen Nutzungsbewilligung. GEOTEAM Internal Report, GEOTEAM, Gleisdorf, 37 pp.

Maloszewski P. and Zuber A., 1996. Lumped parameter models for the interpretation of environmental tracer data. Manual on Mathematical Models in Isotope Hydrogeology, IAEA-TECDOC-910, International Atomic Energy Agency, Vienna, 9-58.

McGuire, K.J. and McDonnell, J.J., 2006. A review and evaluation of catchment transit time modeling. Journal of Hydrology, 330/3-4, 543–563. http://dx.doi.org/10.1016/j.hydrol.2006.04.020

Neunteufel, R., Schmidt, B. and Perfler, R., 2016. Wasserversorgung im Jahre 2015 Erfahrungen und Ausblick. Institut für Siedlungswasserbau, Industriewasserwirtschaft und Gewässerschutz, Department Wasser-Atmosphäre-Umwelt, Universität für Bodenkultur Internal Report, Wien, 126 pp.

Nowotny, A., Herrmann, P., Kreuss, O., Heinrich, M. and Magiera, J., 2002. Provisorische Geologische Karte 1:50.000, 107 Mattersburg, Geologische Bundesanstalt, Wien.

Pfleiderer S., Untersweg, T., Benold, C., Leis, A., Rabeder, J., Reitner, H. and Heinrich, M., 2015. Hydrogeologische Grundlagen und Detailcharakterisierungen sowie integrative Auswertungen geologischer, tektonischer und geochemischer Aspekte der Wasserhöffigkeit und des Grundwasserschutzes in den penninischen, zentralalpinen und jungen geologischen Einheiten der südöstlichen Buckligen Welt. Geological Survey of Austria Internal Report, Geologische Bundesanstalt, Wien, 142 pp.

Pirkl, H., Schedl, A. and Pfleiderer, S. (eds.), 2015. Geochemischer Atlas von Österreich – Bundesweite Bach- und Flusssedimentgeochemie (1978–2010). Archiv für Lagerstättenforschung, 28, Geologische Bundesanstalt, Wien, 288 pp.

Schnabel, W. (ed.), Fuchs, G., Matura, A., Bryda, G., Egger, J., Krenmayr, H.G., Mandl, G.W., Nowotny, A., Roetzel, R., Schna-

bel, W. and Scharbert, S., 2002. Geologische Karte von Niederösterreich 1:200.000 mit Legende und Kurzerläuterung. Geologische Bundesanstalt / Land Niederösterreich, Wien.

Schubert, G., Lampl, H., Shadlau, S. and Wurm, M., 2003. Hydrogeologische Karte von Österreich 1:500.000. Geologische Bundesanstalt, 1 Blatt, Wien.

Schuster, R., 2015. Zur Geologie der Ostalpen. Abhandlungen der Geologischen Bundesanstalt, 64, 143–165.

Skoda, G. and Lorenz, P., 2003. Mittlere Jahresniederschlagshöhe. in: BMLFUW (ed.), Hydrologischer Atlas Österreichs, 1. Lieferung. Kartentafel 2.2 Bundesministerium für Land- und Forstwirtschaft, Umwelt und Wasserwirtschaft, Wien.

Stadtnachrichten Kirchschlag, 2016. Trinkwasserzukunft Bucklige Welt. Stadtnachrichten Kirchschlag in der Buckligen Welt, 218, 2.

Suette, G. and Zojer, H., 2005. Wasserprojekt Wechsel. Optimierung der Trinkwassernutzung und des Hochwasserschutzes. Projekt Phase I. Amt d. Steiermärkischen Landesregierung und Amt der Niederösterreichischen Landesregierung Internal Report, Graz, 54 pp.

Trinkwasserverordnung, 2001. Verordnung des Bundesministers für soziale Sicherheit und Generationen über die Qualität von Wasser für den menschlichen Gebrauch. Bundesgesetzblatt II, 304, 1805–1822.

Tukey, J.W., 1977. Exploratory data analysis. Addison-Wesley Publishing Company, 688 pp.

Wasserdatenverbund NÖ: Online-Abfrage des Wasserbuchs beim Amt der Niederösterreichischen Landesregierung – digitales Informationsverbundsystem. http://www.noe.gv.at/Umwelt/ Wasser/Wasserbuch-Online/WDV_OnlineAbfrage.html. (accessed 26 November 2015)

Wasserstandsnachrichten NÖ: Online-Abfrage der Wasserstandsnachrichten und Hochwasserprognosen beim Amt der Niederösterreichischen Landesregierung – digitales Informationsverbundsystem. http://noel.gv.at/wasserstand/static/stations/210302/station.html. (accessed 26 November 2015)

Wessely, G. (ed.), Draxler, I., Gangl, P., Gottschling, P., Heinrich, M., Hofmann, T., Lenhardt, W., Matura, A., Pavuza, R., Peresson, H. and Sauer, R., 2006. Niederösterreich Geologie der österreichischen Bundesländer. Geologische Bundesanstalt, Wien, 416 pp.

WHO, 2011. Guidelines for drinking-water quality (4th ed.). World Health Organisation, Geneva, 541 pp.

Sebastian PFLEIDERER[1)*)], Heinz REITNER[1)] & Albrecht LEIS[2)]

[1)] Geological Survey of Austria, Neulinggasse 38, 1030 Vienna, Austria;

[2)] JR-AquaConSol GmbH, Steyrergasse 21, 8010 Graz, Austria;

[*)] Corresponding author, sebastian.pfleiderer@geologie.ac.at